

ANALYSIS OF SURFACE CONTAMINANTS IN BIOLOGICAL
SAMPLES BY CHARACTERISTIC X-RAY ANALYSIS

by

MONTY O. VOLCKMANN

B. S., Southwest Missouri State College, 1970

9589

A MASTER'S THESIS

submitted in partial fulfillment of the

requirements for the degree

MASTER OF SCIENCE

Department of Physics

KANSAS STATE UNIVERSITY
Manhattan, Kansas

1972

Approved by:

J. J. Seeman
Major Professor

LD
2668
T4
1972
V63
c.2

ii

TABLE OF CONTENTS

	PAGE
LIST OF TABLES	iii
LIST OF PLATES	iv
CHAPTER	
I. INTRODUCTION	1
II. X-RAY TRANSITIONS AND K-SHELL IONIZATION CROSS SECTION	3
III. EXPERIMENTAL PROCEDURE	15
IV. EXPERIMENTAL RESULTS	23
V. ERROR CALCULATION	43
VI. CONCLUSION	44
REFERENCES	46
ACKNOWLEDGMENTS	47
ABSTRACT	

LIST OF TABLES

TABLE	PAGE
I. K-series X-ray energies and relative intensities for lead and mercury	7
II. L-series X-ray energies for lead	10
III. L-series X-ray energies for mercury	11

LIST OF PLATES

PLATE	PAGE
I. A diagram of K-series X-ray transitions	6
II. A diagram of L-series X-ray transitions	9
III. The total cross section for K-shell ionization as a function of incident energy for a screening number $\sigma_K=0.85$	14
IV. A schematic of the target chamber and detector location	19
V. A block diagram of electronics	22
VI. Spectrum obtained from .01% Pb flour target with 18 Mev 4+ oxygen-16 beam	25
VII. Spectrum obtained from 1% Pb flour target with 18 Mev 4+ carbon-12 beam	27
VIII. Spectrum obtained from 1% Pb flour target with 2 Mev proton beam	29
IX. Spectrum obtained from 1% Pb flour target with 8 Mev proton beam	31
X. Spectrum obtained from 1% Hg flour target with 4.4 Mev proton beam	33
XI. Spectrum obtained from 1% Pb flour target with 4.4 Mev proton beam	35
XII. Spectrum obtained from 1% Pb and 1% Hg flour target with 4.4 Mev proton beam	37
XIII. Spectrum obtained from .01% Pb flour target with 4.6 Mev proton beam	40

CHAPTER I

INTRODUCTION

A technique is presented for the quantitative and qualitative determination of contaminants in food substances. The technique is based upon observations of characteristic K-series X-rays resulting from charged particle bombardment of thick targets of the substance. A determination of the heavy element contaminants in flour samples is presented as an illustration of this technique.

Characteristic X-ray analysis has an advantage over recoil particle analysis which recently has been employed in the analysis of flour samples.¹ By using X-ray analysis, it is possible both to detect and to positively distinguish between lead and mercury contaminants. By using recoil particle analysis it is possible to detect but is very difficult to distinguish between these contaminants because of their small mass separation.

When a target is bombarded by an ion beam, two kinds of radiation are emitted. One type, known as characteristic X-ray radiation, consists of discrete spectral lines whose frequencies are characteristic of the atoms forming the target. The other type has a continuous spectrum and is known as Bremsstrahlung. Bremsstrahlung radiation comes from the sudden deceleration of the ion beam colliding with the target atoms. The amount of Bremsstrahlung radiation produced by protons or heavier ions is small in comparison with that produced by electrons because these heavier particles take longer to slow down in the target. Only characteristic X-ray radiation is of direct interest for the determining of trace elements in a target.

Food substances are essentially composed of hydrogen, oxygen, carbon, and nitrogen. These elements are the major constituents of proteins,² and carbohydrates.³ Characteristic X-rays from these elements lie below 0.531 keV,⁴ while some resulting from contaminants such as lead and mercury have energies well above 15 keV. Consequently, it is possible to detect these contaminants without interference from the major constituents by using a Ge(Li) detector which has a lower detection energy limit of approximately 15 keV. A Ge(Li) detector with a resolution of approximately 1.4 keV was used in the experiment to look at the characteristic X-ray spectra from thick targets of flour. Thick targets were employed because biological substances are more conveniently prepared for analysis in this form.

CHAPTER II

X-RAY TRANSITIONS AND K-SHELL IONIZATION CROSS SECTION

A simple explanation of characteristic X-ray production is as follows. An electron in an inner shell of an atom can only be excited to a level that is not occupied by other electrons. The electron must therefore be excited to one of the optical levels of the atom, or it must be excited to one of the continuous levels of positive energy. On the scale of X-ray energies, the whole energy range of optical levels is so small that they may be neglected unless finer details are being detected.⁵ The process of excitation, therefore, consists of ejecting the electron from one of the closed shells thus leaving the resulting atomic ion in a highly excited state.

When a K-electron is ejected, an electron from one of the outer shells, such as the L, M, N, or O shell, can then jump to the free state $n=1$ emitting one of the K-series characteristic X-rays. The frequency of the emitted X-ray will be given by the difference in energy of the K-shell and the shell from which the electron jumped to fill the vacancy. In a similar way the removal of an electron from either the L or M shell gives rise to respectively the L-series and the M-series.

The emission of the K-series X-rays must always be accompanied by the simultaneous emission of the other X-ray series. This is readily apparent, since the vacancies created by the emission of the K-series spectrum from the L, M, and N shells also leaves vacancies in these shells. These vacancies in turn give rise to the M-series and N-series. The M and N-series only

appear in atoms of medium and large atomic number in which the corresponding outer shells are also partially or fully filled.

The general rule as to whether or not a transition is allowed is that $\Delta l = \pm 1$ and $\Delta j = 0, \pm 1$.⁶ All other transitions correspond to forbidden transitions. Such forbidden transitions are not absolutely prohibited, but their probability of occurrence is at least 10^6 times smaller than the allowed transitions.⁷ There is no selection rule restricting the possible changes in the quantum number n .

Plate I shows the different K-series X-ray energy transitions and their designations.⁸ Table I gives the K-series X-ray energies for lead and mercury.⁹ Plate II shows the different L-series X-ray energy transitions and their designations.¹⁰ Tables II and III give the L-series X-ray energies respectively for lead and mercury.¹¹

The $K'_{\beta 1}$ series consists of three different transitions, while the $K'_{\beta 2}$ series consists of two different transitions. The $K_{\alpha 1}$ and $K_{\alpha 2}$ series each consist of only one transition. The most intense K-series X-ray is the $K_{\alpha 1}$, followed in decreasing order of intensity by the $K_{\alpha 2}$, the $K'_{\beta 1}$; and the $K'_{\beta 2}$ series.

The L-series gets its name in the same way that the K-series does. In this case an L-shell vacancy, instead of a K-shell vacancy, is filled by an electron from a higher energy shell. Since the L shell is split into two different energy levels, there will be more possible X-rays associated with it.

The low energy approximation to the cross section as given by the Born approximation¹² is $\sigma_K \approx \frac{2^{20} \pi^2 m^4 E^4 a_0^2}{45 M^4 Z^{12}}$. The quantity M is the

**THIS BOOK
CONTAINS
NUMEROUS PAGES
THAT WERE
BOUND WITHOUT
PAGE NUMBERS.**

**THIS IS AS
RECEIVED FROM
CUSTOMER.**

EXPLANATION OF PLATE I

FIG. 1. A diagram of K-series X-ray Transitions.

**THIS BOOK
CONTAINS
NUMEROUS PAGES
WITH DIAGRAMS
THAT ARE CROOKED
COMPARED TO THE
REST OF THE
INFORMATION ON
THE PAGE.**

**THIS IS AS
RECEIVED FROM
CUSTOMER.**

PLATE I

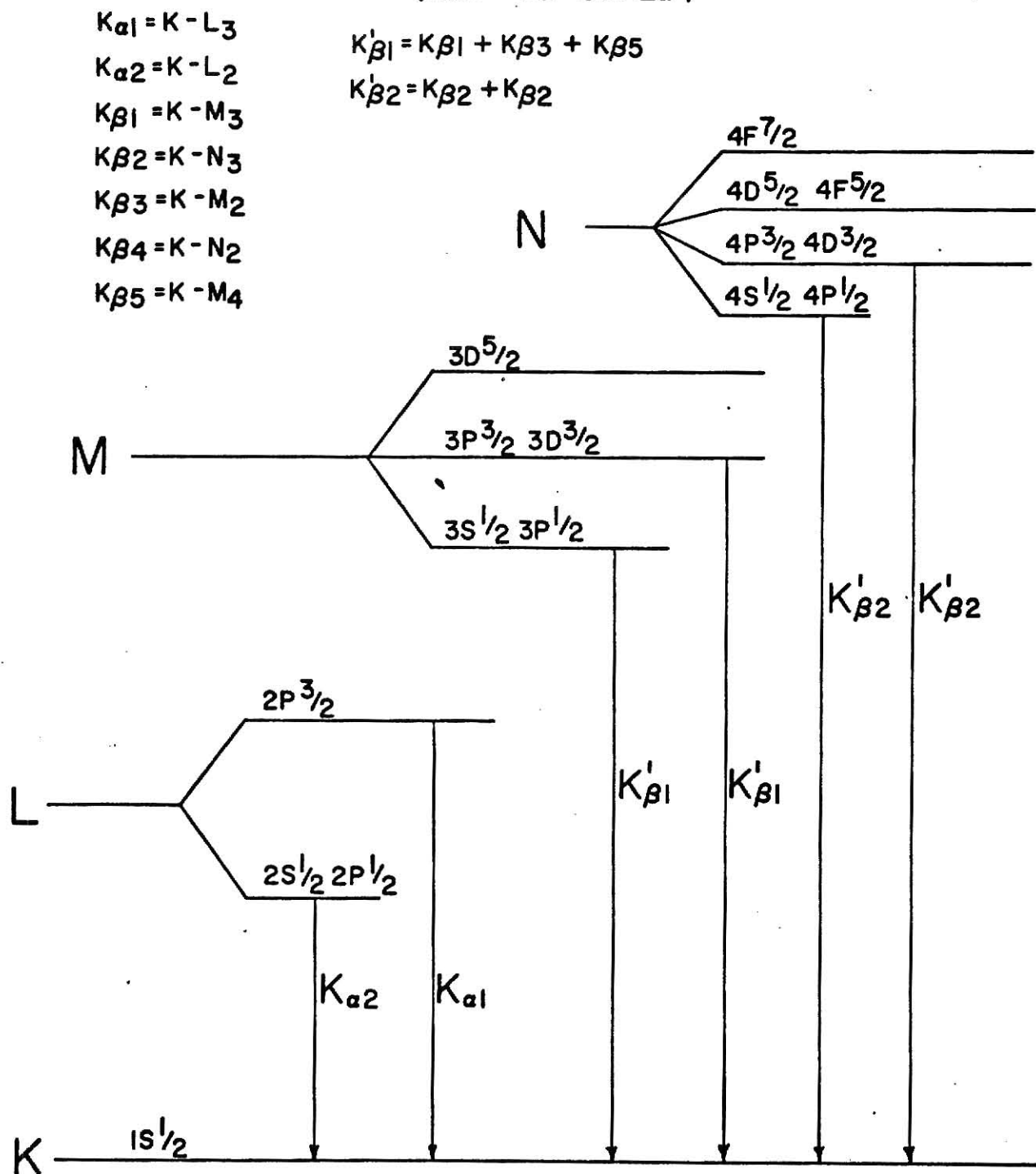
K SERIES X-RAY ENERGY TRANSITIONS
(NOT TO SCALE)

TABLE I

Lead

<u>Designation</u>	<u>X-ray Energy in keV</u>	<u>Relative Intensity</u>
$K_{\alpha 2}$	72.80	55
$K_{\alpha 1}$	74.97	100
$K_{\beta 1}$	84.936	
$K_{\beta 3}$	84.450	
$K_{\beta 5}$	85.43	
$K'_{\beta 1}$	84.8	35
$K_{\beta 2}$	87.364	
$K_{\beta 4}$	87.23	
$K'_{\beta 2}$	87.3	10

Mercury

<u>Designation</u>	<u>X-ray Energy in keV</u>	<u>Relative Intensity</u>
$K_{\alpha 2}$	68.89	55
$K_{\alpha 1}$	70.82	100
$K_{\beta 1}$	80.253	
$K_{\beta 3}$	79.822	
$K_{\beta 5}$	80.75	
$K'_{\beta 1}$	80.2	35
$K_{\beta 2}$	82.54	
$K_{\beta 4}$	82.43	
$K'_{\beta 2}$	82.5	10

Identification of Different Levels in Different Shells

	K	L _I	L _{II}	L _{III}	M _I	M _{II}	M _{III}	M _{IV}	M _V
	1S $\frac{1}{2}$	2S $\frac{1}{2}$	2P $\frac{1}{2}$	2P $\frac{3}{2}$	3S $\frac{1}{2}$	3P $\frac{1}{2}$	3P $\frac{3}{2}$	3D $\frac{3}{2}$	3D $\frac{5}{2}$
n=	1	2	2	2	3	3	3	3	3

EXPLANATION OF PLATE II

FIG. 2. A diagram of L-series X-ray Transitions.

PLATE II

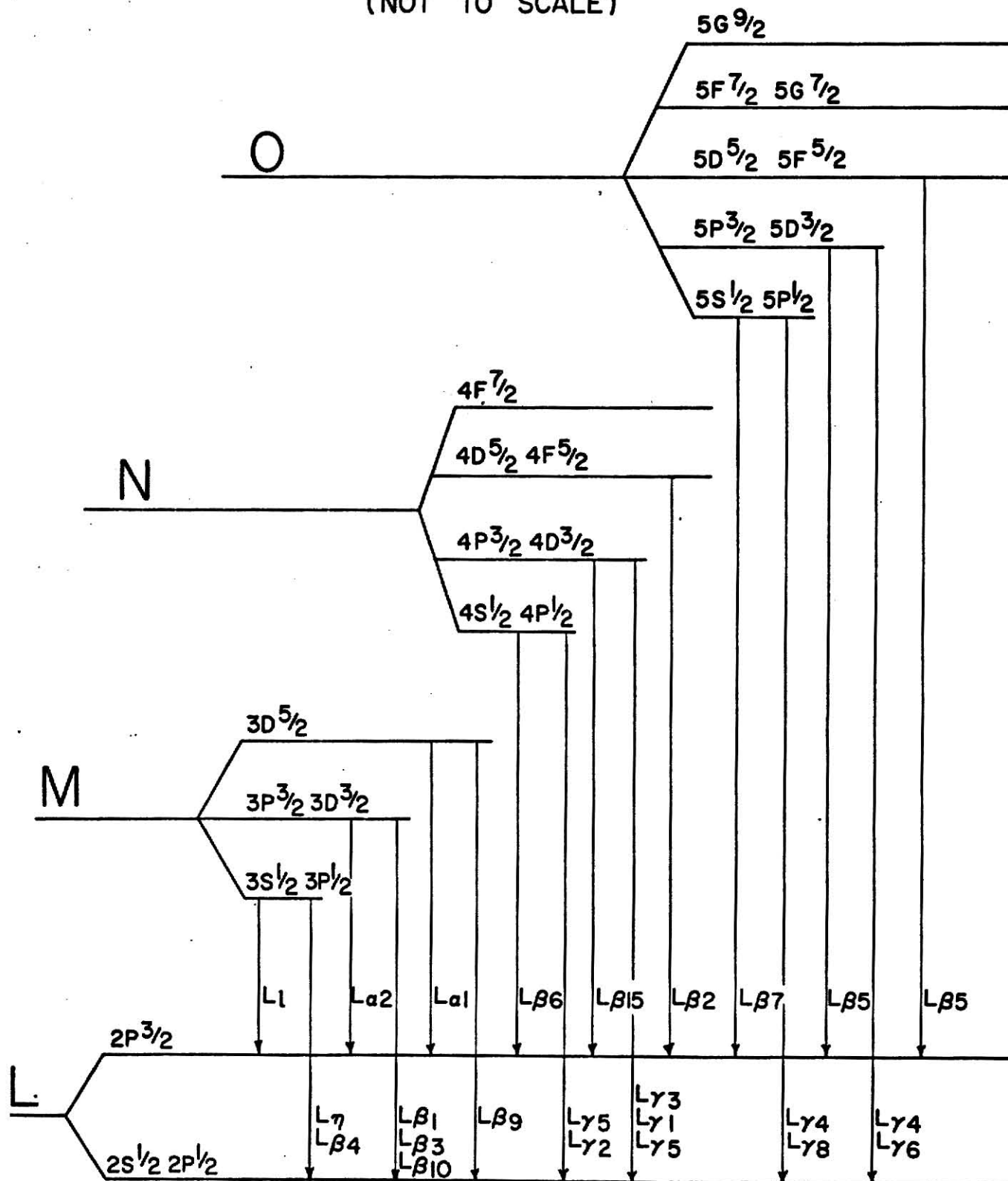
L SERIES X-RAY ENERGY TRANSITIONS
(NOT TO SCALE)

Table II. L-Series X-ray Data of Lead

Designation	X-ray Energy in Kev
β_4 L_{II}^{MII}	12.306
β_3 $L_{I}^{M_{III}}$	12.7933
γ_2 $L_{I}^{N_{II}}$	15.101
γ_3 $L_{I}^{N_{III}}$	15.218
γ_4' $L_{I}^{O_{II}}$	15.752
γ_4 $L_{I}^{O_{III}}$	15.777
η $L_{II}^{M_I}$	11.3493
β_1 $L_{II}^{M_{IV}}$	12.6137
γ_5 $L_{II}^{N_I}$	14.3075
γ_1 $L_{II}^{N_{IV}}$	14.7644
γ_8 $L_{II}^{O_I}$	15.0527
γ_6 $L_{II}^{O_{IV}}$	15.1783
ζ $L_{III}^{M_I}$	9.1845
α_3 $L_{III}^{M_{IV}}$	10.4495
α_1 $L_{III}^{M_V}$	10.5515
β_6 $L_{III}^{N_I}$	12.143
β_{15} $L_{III}^{N_{IV}}$	12.6011
β_2 $L_{III}^{N_V}$	12.6226
β_7 $L_{III}^{O_I}$	12.888
β_8 $L_{III}^{O_{IV,V}}$	13.015
β_{10} $L_{I}^{M_{IV}}$	13.275
β_9 $L_{I}^{M_V}$	13.377
γ_{11} $L_{I}^{N_V}$	15.453
β_{12} $L_{II}^{M_{III}}$	12.127
ν $L_{II}^{N_{VI}}$	15.060
ϵ $L_{III}^{M_{II}}$	9.4811
ς $L_{III}^{M_{III}}$	9.9675
\mathcal{U} $L_{III}^{N_{VI,VII}}$	12.8968

Table III. L-Series X-ray Data of Mercury

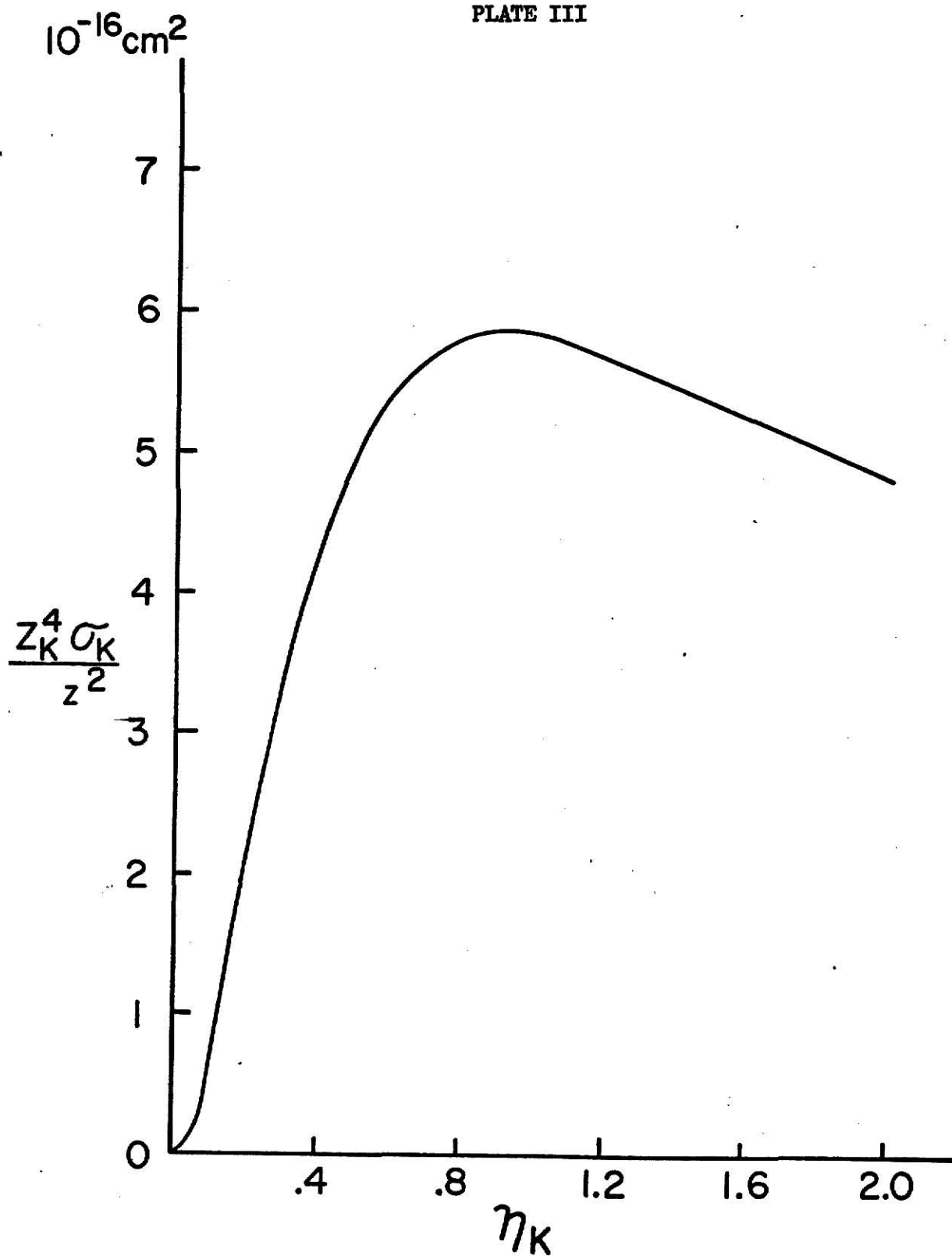
<u>Designation</u>	<u>X-ray Energy in Kev</u>
β_4 L_{I}^{MII}	11.5630
γ_2 L_{IN}^{II}	14.162
γ_3 L_{IN}^{III}	14.265
γ_4' L_{I}^{OII}	14.757
γ_4 L_{I}^{OIII}	14.778
η L_{II}^{MI}	10.6512
β_1 L_{II}^{MIV}	11.8226
γ_5 L_{II}^{NI}	13.410
γ_2 L_{II}^{NIV}	13.8301
γ_8 L_{II}^{OI}	14.090
γ_6 L_{II}^{OIV}	14.199
ζ L_{III}^{MI}	8.7210
α_2 L_{III}^{MIV}	9.8976
α_1 L_{III}^{MV}	9.9888
β_6 L_{III}^{NI}	11.4824
β_{15} L_{III}^{NIV}	11.9040
β_2 L_{III}^{NV}	11.9241
β_7 L_{III}^{OI}	12.1625
β_5 $L_{III}^{OIV,V}$	12.2769
β_{10} L_{I}^{MIV}	12.446
β_9 L_{I}^{MV}	12.560
γ_{11} L_{I}^{NV}	14.474
β_{17} L_{II}^{MIII}	11.358
ν L_{II}^{NVI}	14.107
t L_{III}^{MII}	9.019
S L_{III}^{MIII}	9.455
\mathcal{U}' L_{III}^{NVI}	12.1826
\mathcal{U} L_{III}^{NVII}	12.1940

mass of the projectile, m is the mass of the electron, Z is the atomic number of the target element, a_0 is the first Bohr radius of hydrogen, ze is the charge of the projectile, and E is the incident energy of the projectile. This simple approximation exhibits the qualitative behavior of the cross section in the energy region where the maximum energy that an incident particle can transfer in a free collision to an electron at rest is much less than the binding energy of the electron in the K-shell. The cross section increases as the fourth power of the incident energy and is inversely proportional to the twelfth power of the atomic number Z of the target element. A more accurate formula for the cross section can be arrived at by taking into account the effect of screening by the inner shells. When this is done, the cross section is found to vary at low energies like the Born approximation, but at higher energies the cross section reaches a maximum and then gradually decreases. Plate III gives the total cross section for K-shell ionization as a function of incident energy for a screening number $\mathcal{Q}_k=0.85$. The quantity \mathcal{Q}_k is related to the effective nuclear charge Z_k , the binding energy I_k , and the shell number k by the relationship $k^2 I_k = \mathcal{Q}_k^2 Z_k^2$ Rydberg. The total cross section for K-shell ionization in lead for 4.0 Mev protons can be computed from Plate III. For example, by using $E=4.0$ Mev and $Z_k=82$, the value 0.024 is obtained for the abscissa in Plate III. For $\mathcal{Q}_k=0.85$ the corresponding value of the ordinate is 0.04. The resulting cross section is 90 millibarns.

EXPLANATION OF PLATE III

FIG. 3. The total cross section for K-shell ionization as a function of incident energy for a screening number $\sigma_K=0.85$.

PLATE III



$$\eta_K = \frac{mE}{MZ_K^2 \text{ RYDBERG}}$$

CHAPTER III

EXPERIMENTAL PROCEDURE

In this experiment K-series characteristic X-rays were detected to determine the amount of heavy element contaminant in the flour sample. Measurements were made only of K-series X-rays because a Ge(Li) detector with a resolution of approximately 1.4 keV was available. As was noted previously, this resolution is adequate for resolving lead and mercury K-series X-rays.

It is the resolution of the detector that determines which series of X-rays can be used to distinguish between lead and mercury. Since the energy difference of the relative peak intensities between the L-series X-rays for lead and mercury differ by only approximately 0.9 keV at the most, it is physically impossible to distinguish between these two peaks with a detector having a resolution of 1.4 keV. In the K-series of lead and mercury there is an energy difference of 4.6 keV between the $K_{\beta 1}$ of lead and the $K_{\beta 1}$ of mercury. With such an energy spread it is possible to distinguish between lead and mercury in the flour sample.

The relative intensity of the various K-series X-rays to each other is another factor to consider in the X-ray spectrum analysis. Some confusion can arise from interferences between K_{α} and K_{β} from adjacent elements and between K and L-series, but in most cases this is not a serious drawback. If the spectrum contains a very strong peak there is also an increased background for neighbouring elements.

The energy of the characteristic X-rays will have some slight

dependence on outer electron configuration. The outer electron configuration is affected by both the physical and the chemical state of the element used as a target.¹³ The projectile will also cause a change in the electron configuration.¹⁴ Protons give the least amount of disturbance of any charged ion to the electron structure and to the electron wave function of the target atoms. The energy shifts mentioned above will have negligible effect on the results of this experiment.

Initially, flour targets were made by mixing the flour, contaminant, and distilled water together and letting the mixture dry on an aluminum target backing. Usually this mixture flowed too freely and would not adhere to the target backing. This problem was resolved by putting the target backing on a small sheet of aluminum foil, and pulling the aluminum foil up around the sides of the target backing to form temporary walls for the mixture until it dried. It was found that unless the targets were allowed to dry slowly in air for two days they would crack badly when placed in a vacuum to finish their drying. After having dried in air for a few days, they were then placed in a vacuum dessicator and left under a vacuum for at least another day. After this lengthy process of drying, the targets would usually come out in one piece, but they wouldn't stick to the target backing. It was found that a drop of polystyrene worked very well as a glue to hold the target to the target backing. Another reason polystyrene was used is that the heaviest element composing it is oxygen, whose K-series X-rays lie below the detection range of the Ge(Li) detector used in this experiment.

For purposes of calibration and for purposes of determining how

small a percentage of contaminant could be detected, small amounts of lead oxide and mercurous nitrate were mixed with flour samples. First, a small amount of the contaminant was measured on a set of analytical balances. Then the corresponding amount of flour needed to give the desired value of contaminant to flour ratio was measured on the analytical balance. Distilled water was then added until the proper consistency was achieved. The liquid mixture was then applied to the target backing and dried.

The best experimental results and the most interesting spectra were obtained with the following targets: one percent lead, one percent mercury, one percent lead and one percent mercury mixed together, and one hundredth percent lead.

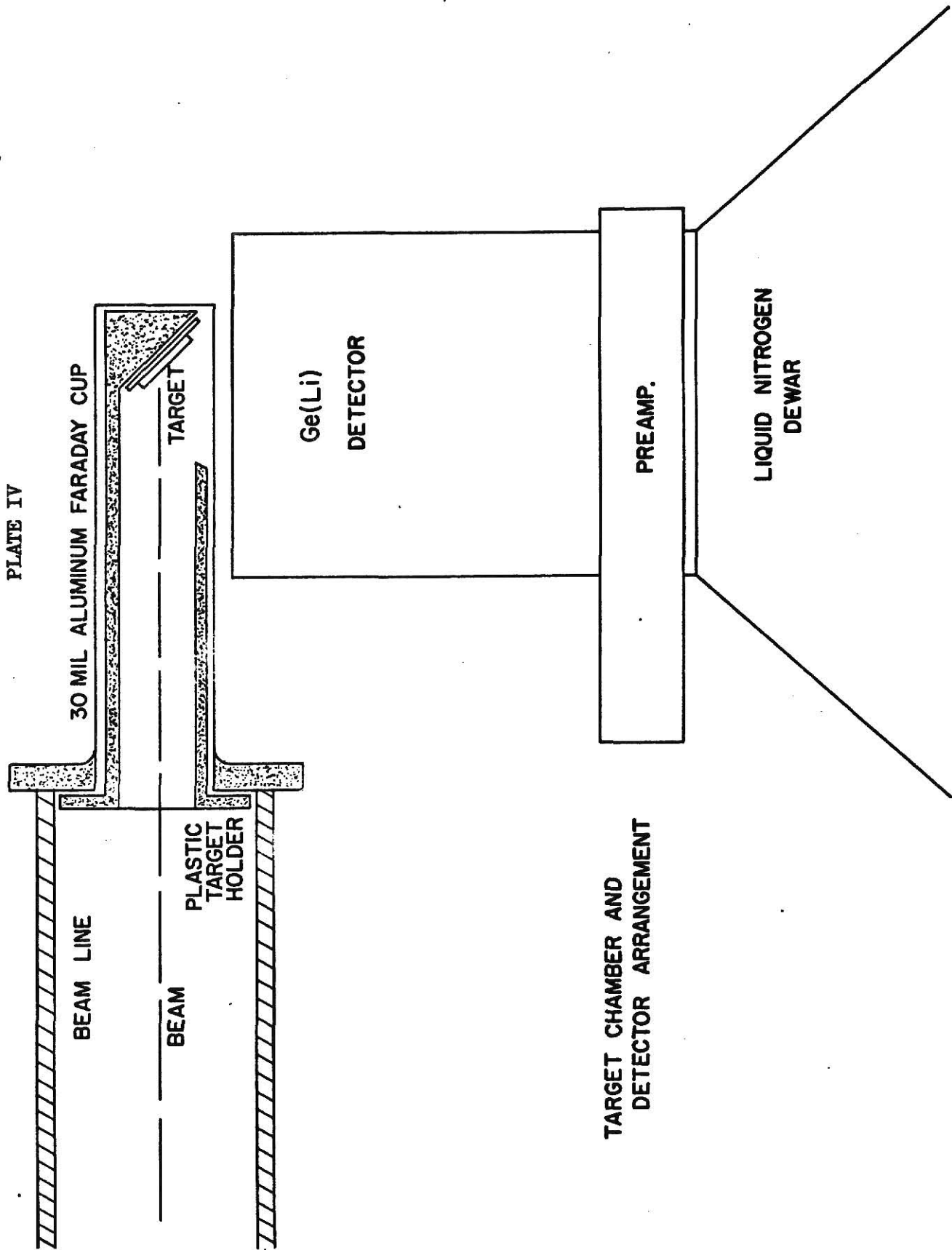
The Ge(Li) detector was placed at approximately ninety degrees to the beam. A schematic of the target chamber and detector location are shown in Plate IV.

Various types of beams of different charge states were produced by the Kansas State University Tandem Van de Graaff accelerator. These included the following: carbon-12 2+ state at 10 Mev, carbon-12 4+ state at 18 Mev, carbon-12 4+ state at 22.3 Mev, oxygen-16 4+ state at 18 Mev, and protons ranging from 2 to 8 Mev. The beam currents varied due to conditions of the source and of the tandem itself. The currents on target ranged from approximately one nanoampere to sixty nanoamperes. Beam currents of more than approximately sixty nanoamperes yielded high counting rates in the Ge(Li) detector and somewhat poorer resolution.

The target current and the total beam current were measured simultaneously in a Faraday cup. In order to get an accurate measurement

EXPLANATION OF PLATE IV

FIG. 4. A schematic of the target chamber and detector location.



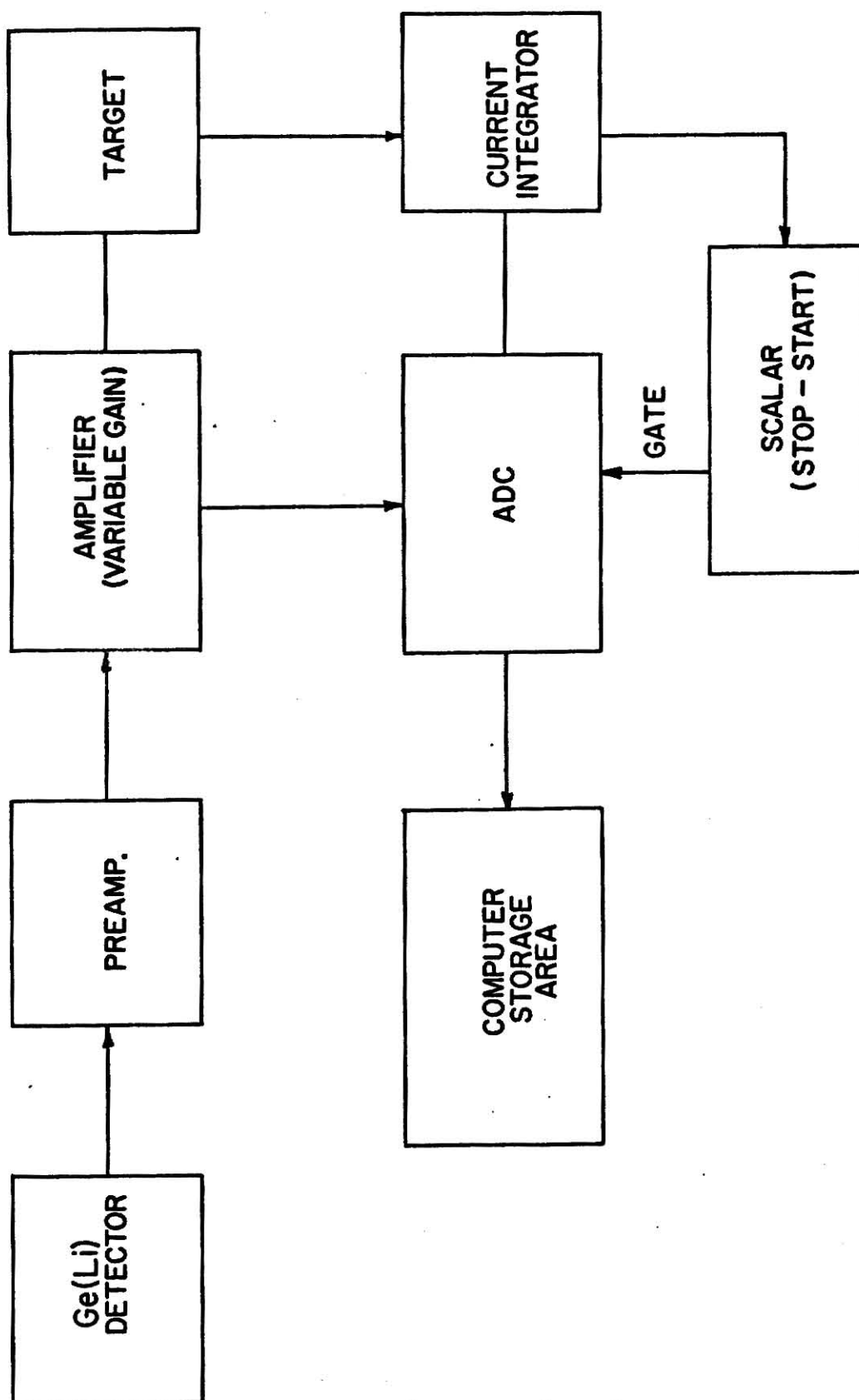
of the beam current it is necessary to use a Faraday cup large enough to collect all the electrons ejected from the target by the incident charged particle.

A block diagram of the electronics used in this experiment is shown in Plate V. Pulses from the detector were amplified with the appropriate gain such that the lead K-series X-rays would lie close to the far right end of the spectrum. The amplified pulse was then routed to the analog-to-digital converter (ADC), which was in turn connected to the multichannel analyzer section of a Digital Equipment Corporation model PDP 15 computer. The beam current on the target was collected and sent to the integrator circuit, which gave a digital pulse proportional to the collected charge on the target. A scaler was then used to record the number of counts from the current integrator. The ADC and the current integrator scaler were started and stopped simultaneously by gating the ADC with a pulse from the scaler when it was turned on.

EXPLANATION OF PLATE V

FIG. 5. A block diagram of electronics.

PLATE V
BLOCK DIAGRAM OF ELECTRONICS



CHAPTER IV

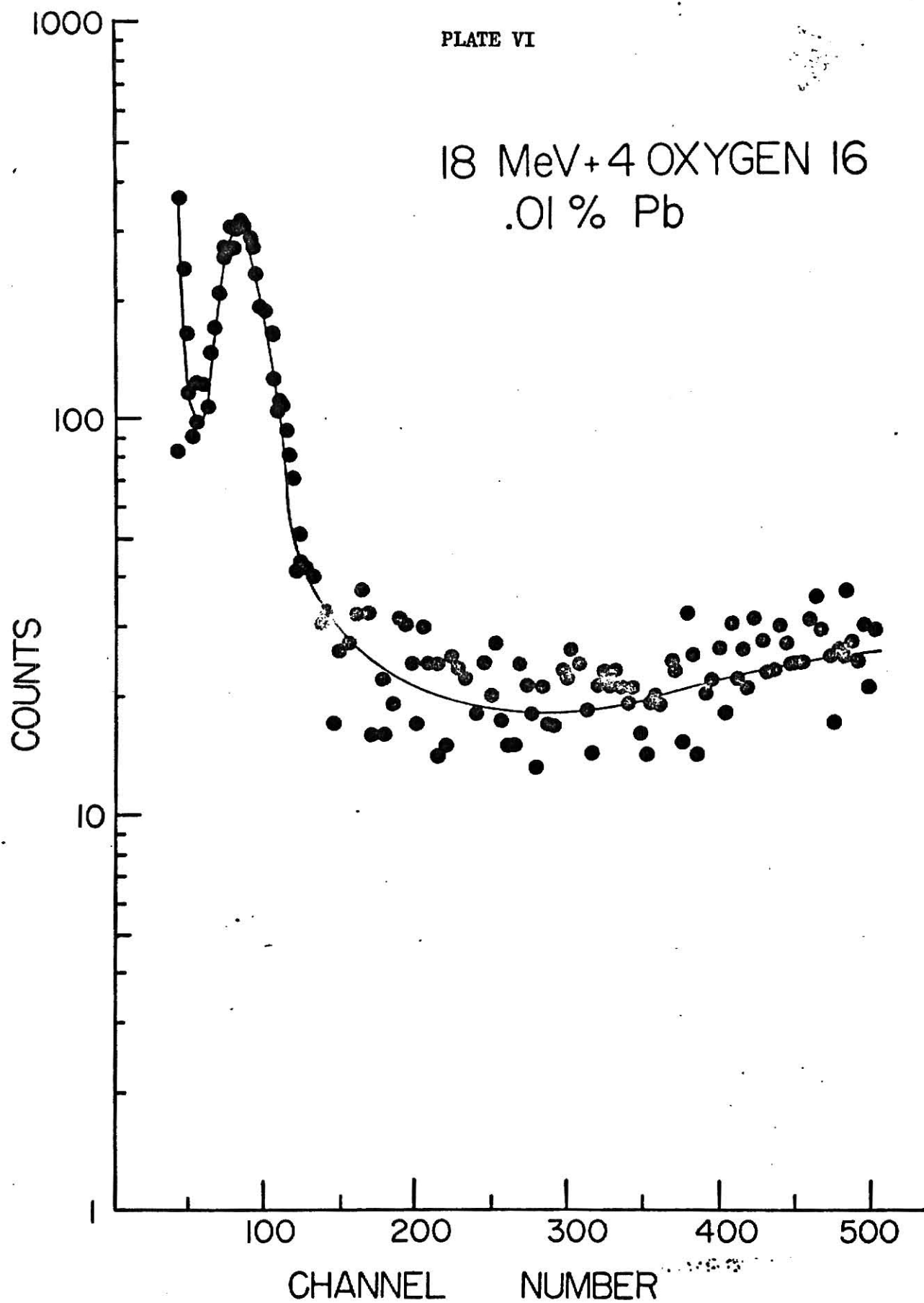
EXPERIMENTAL RESULTS

Plate VI shows the X-ray spectrum obtained with an ^{16}O beam from a 0.01 percent lead target. Plate VII shows the X-ray spectrum obtained with a ^{12}C beam from a one percent lead target. Plates VIII and IX show the spectra obtained respectively with protons of energies 2 and 8 Mev on a one percent lead target. Plate X shows the spectrum obtained with a 4.4 Mev proton beam from a one percent mercury target. Plate XI shows the spectrum obtained with a 4.4 Mev proton beam from a one percent lead target. Initially, different kinds of ion beams were tried to determine which would give the largest ratio of $K_{\beta 1}$ X-ray peak to background. Oxygen and carbon were tried at various energies. The best ratio of peak to background that could be attained was only about two-to-one. With protons, it was found that the best peak to background ratio that could be attained was about ten-to-one with approximately 4.6 Mev protons. For this and other reasons explained below, protons were used in the experiment.

To determine if mercury could actually be resolved from lead, 4.4 Mev protons were run on a target of one percent lead and one percent mercury. As explained earlier, the $K_{\beta 1}$ X-ray is the best one to use to detect mercury when lead is present. The $K_{\beta 1}$ X-ray peak of mercury can definitely be seen on Plate XII at channel number 490. It will be noticed on Plate XII that the $K_{\beta 1}$ peak of mercury is much smaller than the lead $K_{\beta 1}$ peak of lead. When 4.4 Mev protons were run on a one percent mercury target, the same effect was also observed. The $K_{\beta 1}$ peak to background ratio was at

EXPLANATION OF PLATE VI

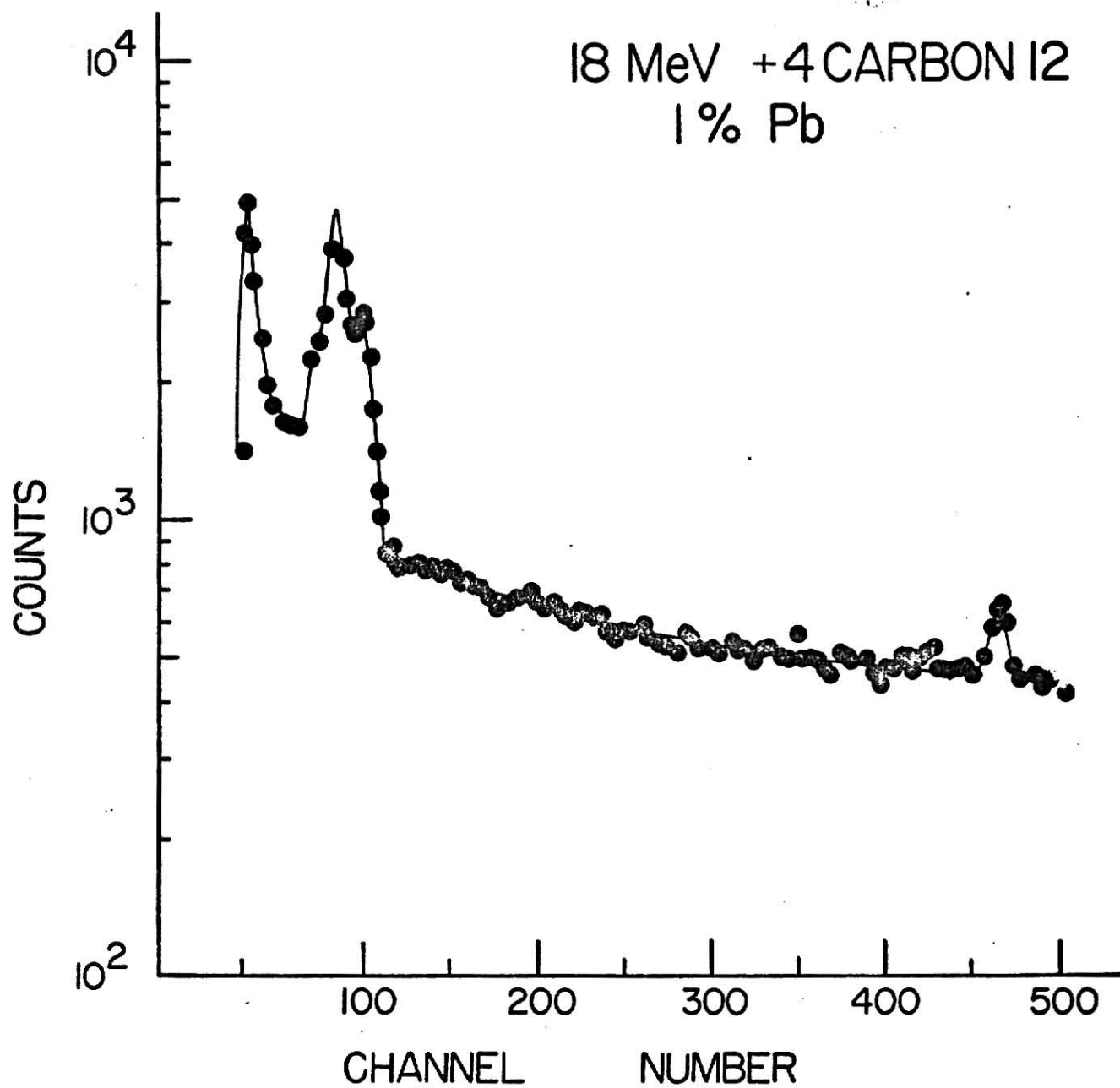
FIG. 6. Spectrum obtained from .01% Pb flour target with 18 Mev
4+ oxygen-16 beam.



EXPLANATION OF PLATE VII

FIG. 7. Spectrum obtained from 1% Pb flour target with 18 Mev 4^+ carbon-12 beam.

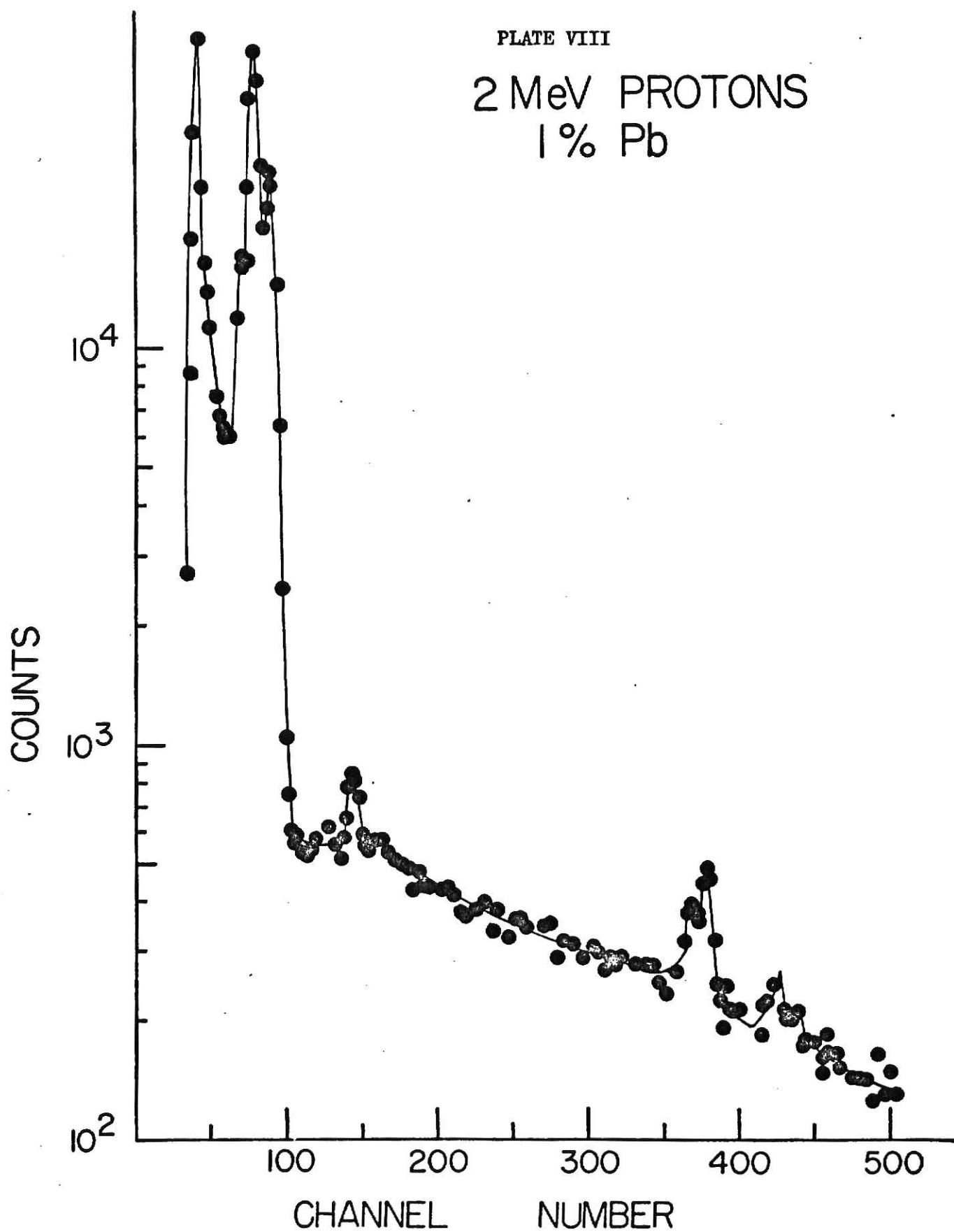
PLATE VII



EXPLANATION OF PLATE VIII

FIG. 8. Spectrum obtained from 1% Pb flour target with 2 Mev proton beam.

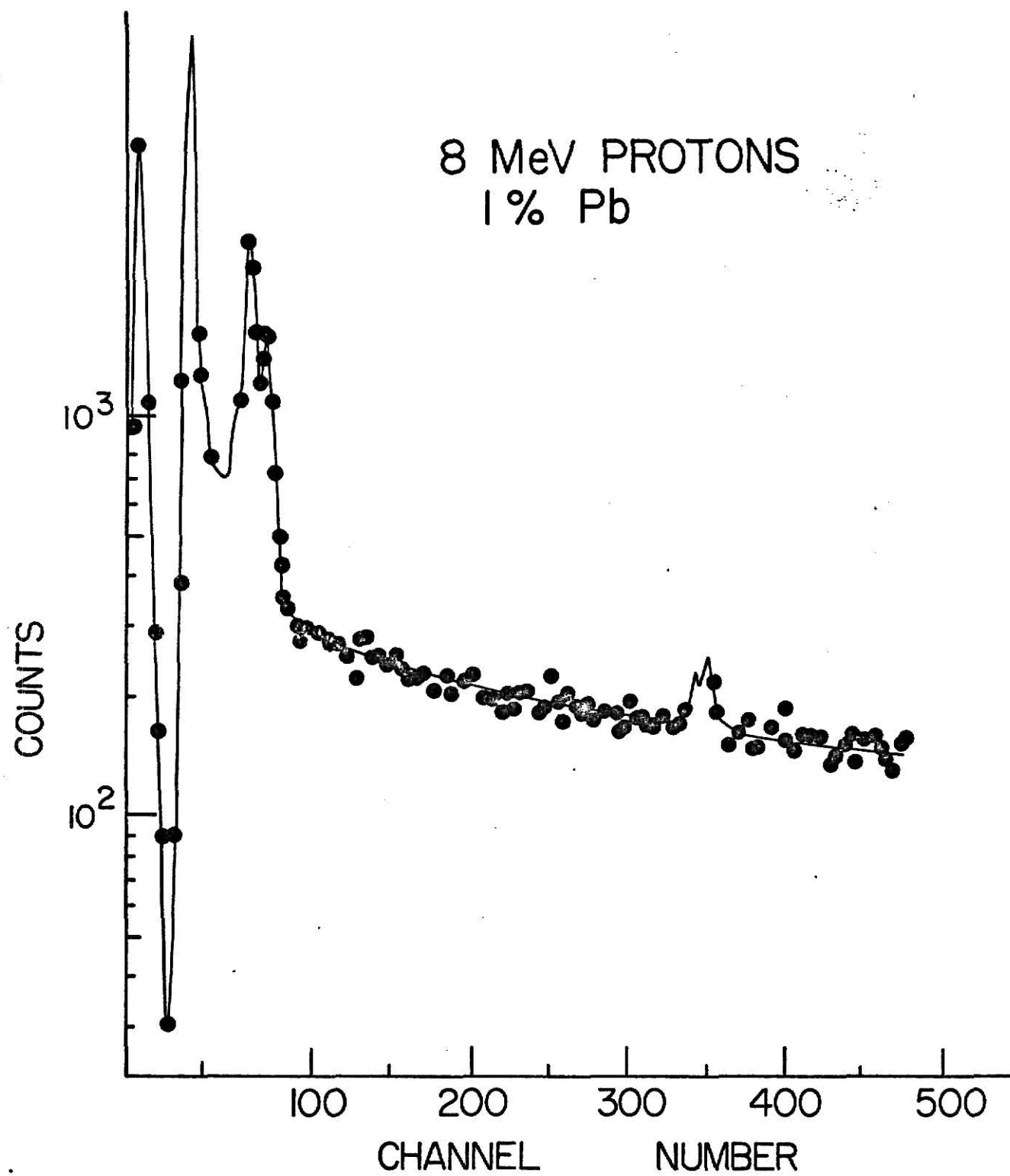
PLATE VIII

2 MeV PROTONS
1% Pb

EXPLANATION OF PLATE IX

FIG. 9. Spectrum obtained from 1% Pb flour target with 8 Mev proton beam.

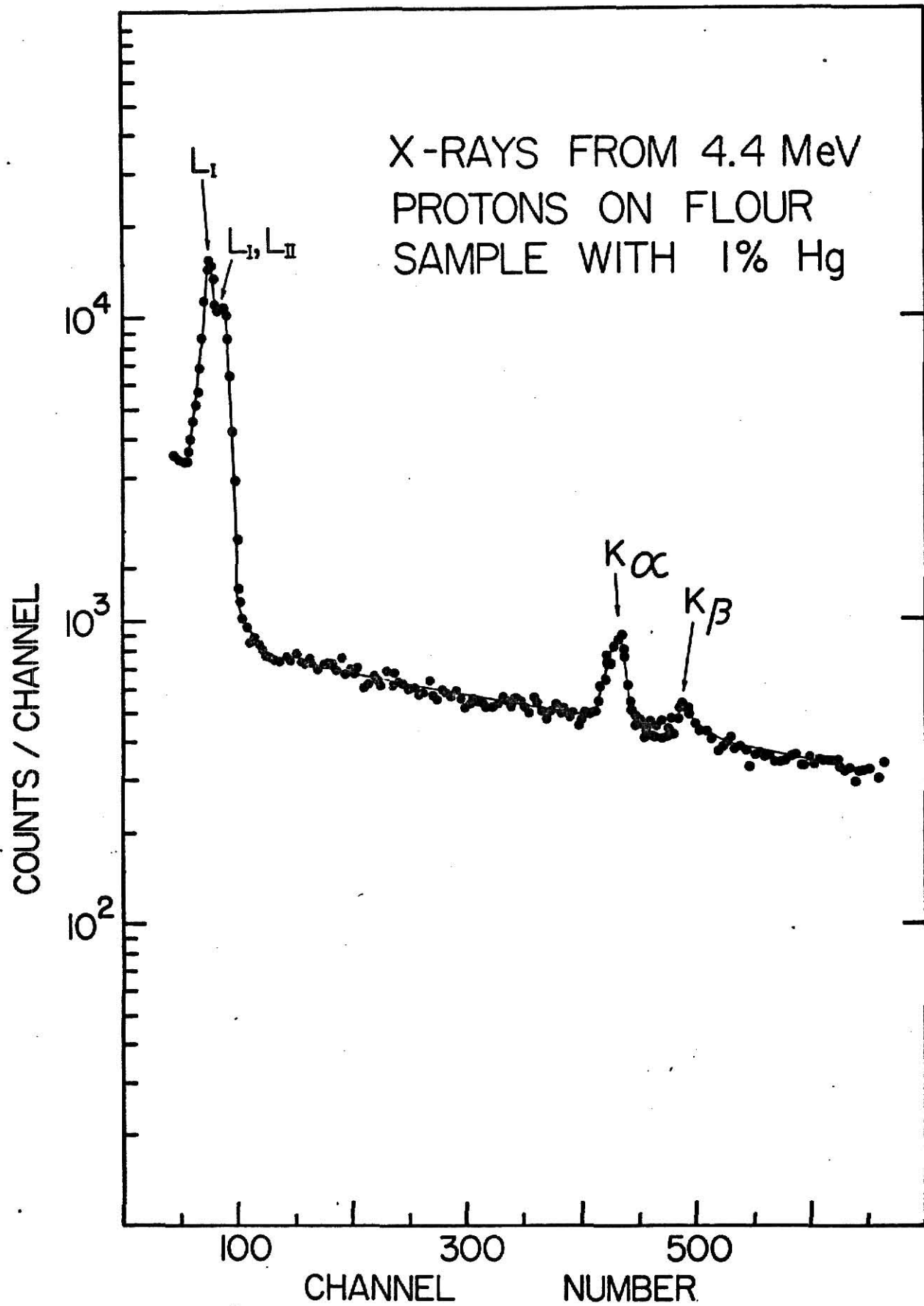
PLATE IX



EXPLANATION OF PLATE X

FIG. 10. Spectrum obtained from 1% Hg flour target with 4.4 Mev proton beam.

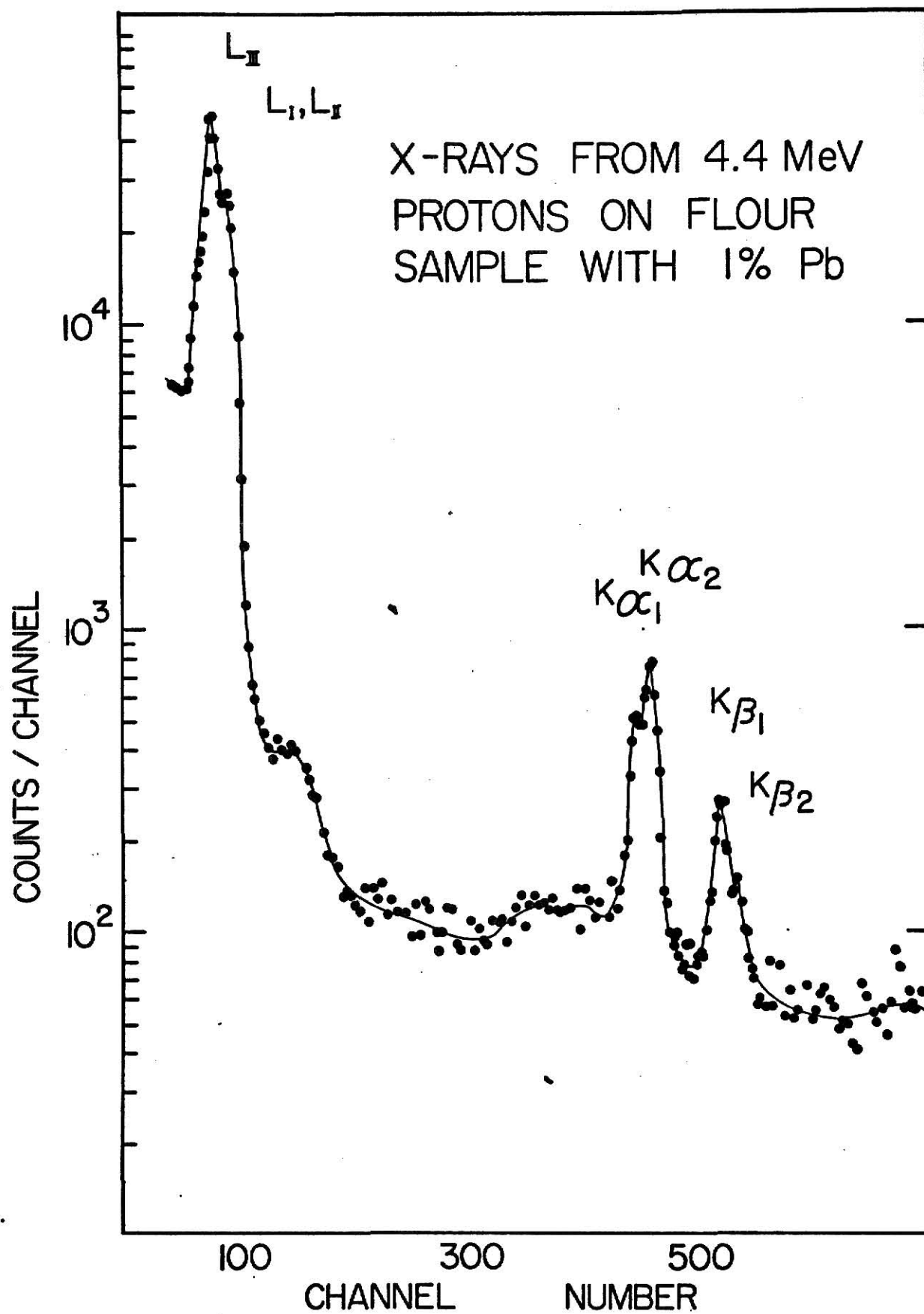
PLATE X



EXPLANATION OF PLATE XI

FIG. 11. Spectrum obtained from 1% Pb flour target with 4.4 Mev proton beam.

PLATE XI

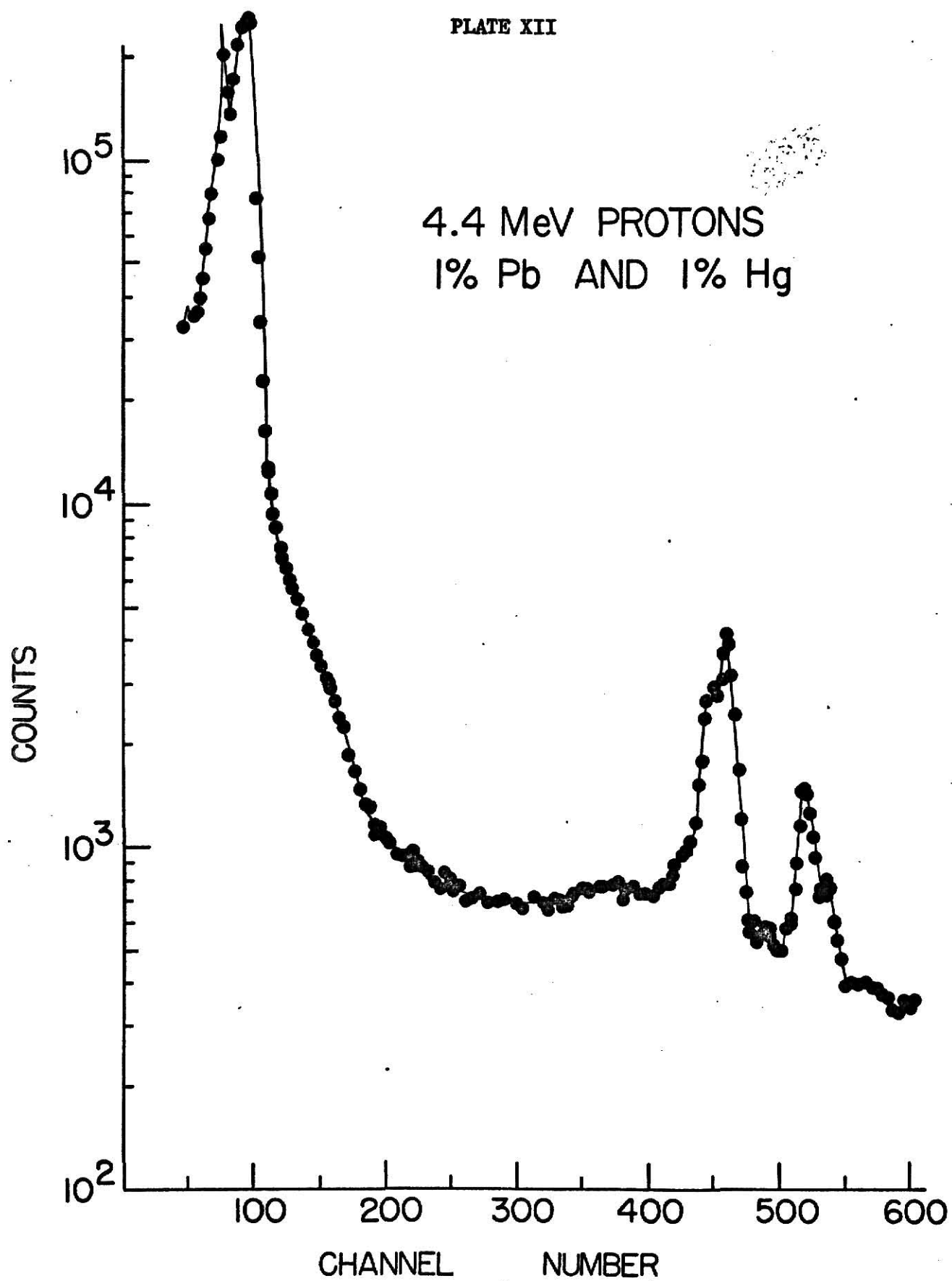


EXPLANATION OF PLATE XII

FIG. 12. Spectrum obtained from 1% Pb and 1% Hg flour target with 4.4 Mev proton beam.

PLATE XII

4.4 MeV PROTONS
1% Pb AND 1% Hg



best only approximately three to one for mercury. This explains why the $K_{\alpha 1}$ peak is so much smaller than the corresponding $K_{\alpha 1}$ peak of lead in the mixed flour target of lead and mercury. However, the mercury in the target can still be distinguished from the lead.

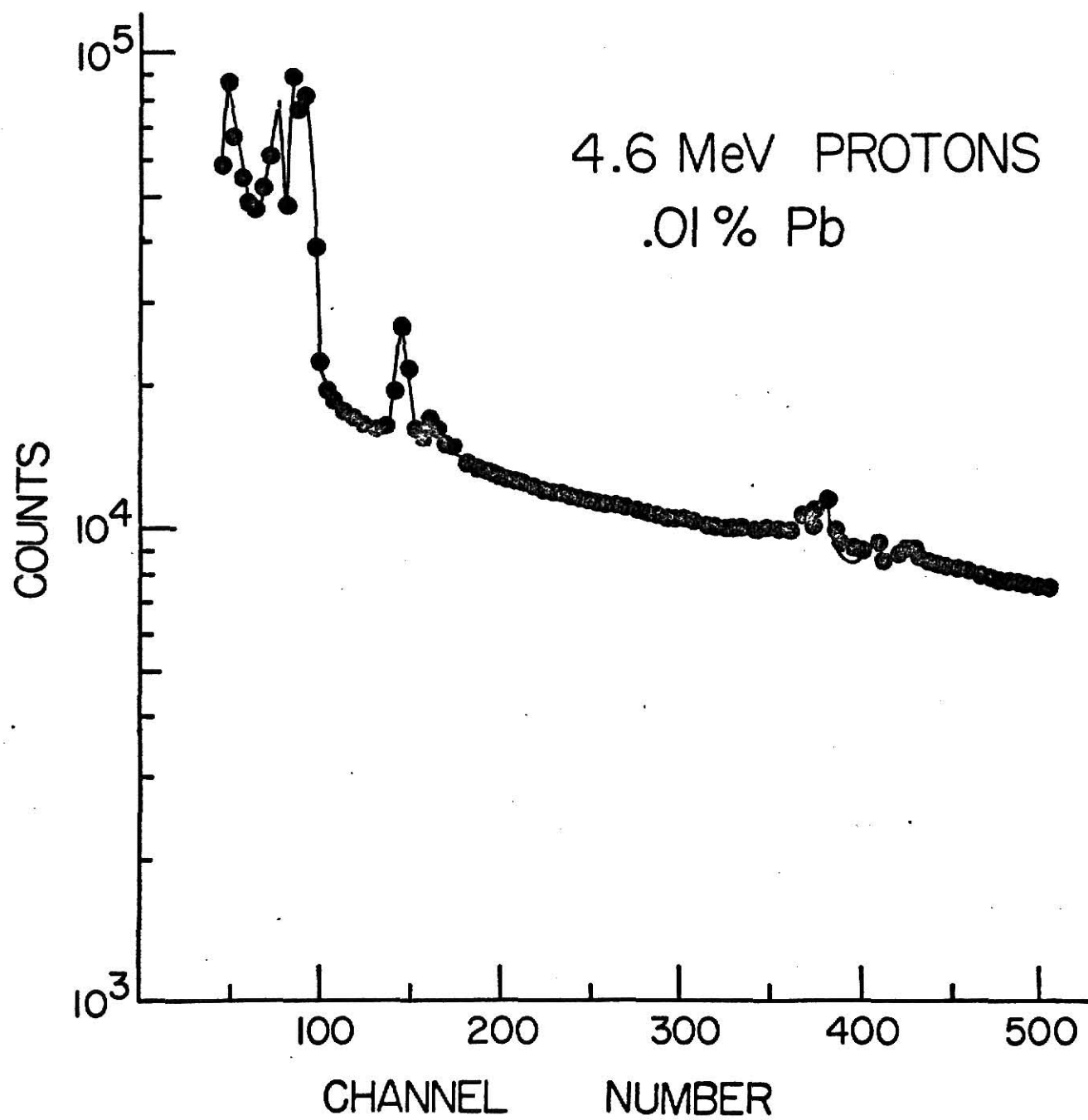
To determine how small an amount of contaminant can be detected with this method, 4.6 Mev protons were then run on a target containing only one hundred parts per million of lead. The $K_{\alpha 1}$ peak of lead can still definitely be resolved in Plate XIII at channel number 380. It appears that the smallest amount of contaminant that can be detected by this technique is of the order of one hundred parts per million, unless the background can be reduced.

Background is the most important limiting factor with this technique. Bremsstrahlung could be one possible source of the large background radiation. Johansson, Akselsson, and Johansson¹⁵ state that Bremsstrahlung radiation is a large part of the background contribution in thick samples. Cross sections for K-series X-rays have been found to be several orders of magnitude larger than those predicted by direct scattering theory for heavy ions.¹⁶ Since the background contribution from Bremsstrahlung radiation is low for heavy ions, it appears that heavy ions should give a far better peak to background ratio.¹⁷ Spectra obtained with heavy ions had higher backgrounds than those obtained from protons. This is illustrated in the plate showing the X-ray spectrum obtained with an oxygen beam. All that can be seen after the L-series X-rays there is just background with no peaks at all. It follows that the large background is not from Bremsstrahlung radiation. Johansson, et al., worked at the 10^{-11}

EXPLANATION OF PLATE XIII

FIG. 13. Spectrum obtained from .01% Pb flour target with 4.6 Mev proton beam.

PLATE XIII



gram level, which could definitely explain why their statements concerning Bremsstrahlung radiation do not seem relevant here. Gamma rays from positron annihilation are the other probable source of such a large background. A gamma ray spectrum taken simultaneously with another detector showed very large 511 keV positron annihilation spectrum. Due to uniform Compton scattering of the 511 keV radiation in the detector, the background would be high and spread out very uniformly over the entire X-ray energy spectrum. Heavy ions make more possible reactions and more daughter nuclei that are positron emitters than do protons. Therefore, heavy ions should produce a larger background than protons. This was observed in this experiment.

Other things were tried to reduce the background contribution in this experiment besides trying different beams at different energies. Different target backings of aluminum, copper, niobium, and tantalum were tried without success. The result was to either increase the background, or in the case of tantalum, to produce K-series X-rays that interfered with the detection of the lead and mercury K-series X-rays. A target backing made out of copper gave the worst spectrum of all backings tried. This can be explained by examining the reaction scheme of copper with protons. The $^{65}\text{Cu}(p,n)$ reaction above 2.13 Mev yields ^{65}Zn which is a positron emitter. The target holder originally was made of brass and it was thought that the beam might be hitting the target and scattering back hitting the brass. A target holder was then made out of plastic since the heaviest element composing it would have K-series X-rays of very low energy. Very little difference could be detected between the spectra obtained with either the plastic or brass target holders.

A thin target was then made by applying the flour mixture to the target backing with a very thin wire mesh attached to the target backing to keep the flour from falling off when it dried. This method of target making was successful, but the spectra obtained from them were not. Aluminum, nickel, and copper wire mesh were used on the target backings to make a thin target of flour. Once again the various metals present in the target backing and wire mesh resulted in large background contributions. Flour on a thin aluminum target backing gave the best spectrum.

An analysis of the background was made. After the beam had been run on a target for a few minutes, a spectrum was taken with the beam for two minutes. The beam was then shut off and another spectrum was taken for two minutes. After an hour without the beam on the target another spectrum was taken for two minutes without the beam. The background had a halflife of approximately ten minutes. At the end of one hour (6 halflives) the background was almost gone. The next question is what has a halflife of approximately ten minutes and is a good positron emitter? Since many different types of target backings were tried and gave very little difference in the spectra, or made them worse, it was concluded that the background must be coming from a reaction of the protons and the target itself.

$^{12}\text{C} + \text{proton} \rightarrow ^{13}\text{N}$ which has a halflife of approximately ten minutes by positron emission to carbon 13. Since flour contains a large percentage of carbon this would explain why all efforts to eliminate the large background were unsuccessful.

CHAPTER V

ERROR CALCULATION

The only substantial error in this experiment comes from the inaccuracy in determining the area under the $K_{\alpha 1}$ and the $K_{\alpha 2}$ peak. The real problem here is how accurately the background can be determined, since it must be subtracted from the total area under the peaks for purposes of calibration. First a background curve is drawn that gives the best fit to the data. This best-fit background-curve is then varied up and down until it clearly does not fit the data. The area between the upper and lower extremes of these curves between the $K_{\alpha 1}$ and $K_{\alpha 2}$ peaks is then taken as a measure of the uncertainty in the area under the peaks. When this method of error calculation is performed, the ratio of uncertainty in background area to $K_{\alpha 1}$ and $K_{\alpha 2}$ peak area is found to be approximately 10%.

Another source of error in this experiment may be the loss of electrons from the Faraday cup resulting in an incorrect current reading. This slight error is negligible for this experiment.

CHAPTER VI

CONCLUSION

This experiment has demonstrated that contaminants of lead and mercury in food substances can be detected both qualitatively and quantitatively by characteristic X-ray analysis following heavy ion bombardment. A sensitivity of 100 parts per million was obtained by observing K X-rays from thick targets of flour. This sensitivity is approximately the same as that obtainable by chemical analysis.

The sensitivity of this technique can be increased by several orders of magnitude by observing L-series X-rays. According to Johansson, et al., the best results for the heavy elements can be obtained by looking at the L-series X-rays.¹⁸ The cross section for L-series X-ray production is at least two to three orders of magnitude larger than the cross section for K-series X-ray production, while the corresponding background will be unchanged. On this account a sensitivity of at least one part in ten million should be obtainable by observing the L-series X-rays.

The L-series X-rays all lie in a much narrower energy region. Consequently, a detector with a smaller resolution will be required. The resolution necessary to distinguish between the L-series X-rays of lead and mercury can be estimated. The largest energy difference between the most prominent peaks of the L-series X-rays of lead and mercury is less than 0.9 keV. Therefore a detector with a resolution of at least 0.25 keV would be desirable.

This technique can be used on all biological samples that are

composed mostly of light elements. Since carbohydrates and proteins are composed exclusively of light elements, this technique can be used on nearly all animal and vegetable food substances. If the sensitivity could be increased, this technique would be useful in determining the amount of heavy element contaminants in food and food substances.

REFERENCES

- 1) J. K. West, Master's Thesis, Kansas State University, 1971 (unpublished).
- 2) R. T. Morrison and R. N. Boyd, Organic Chemistry (Allyn and Bacon, Inc., Massachusetts, 1966), 2nd ed., p. 1098.
- 3) J. D. Roberts, R. Stewart, and M. C. Caserio, Organic Chemistry (W. A. Benjamin, Inc., New York, 1971), p. 399.
- 4) F. Ajzenberg-Selove, Nuclear Spectroscopy (Academic Press, Inc., New York, 1960), p. 214.
- 5) H. G. Kuhn, Atomic Spectra (Academic Press, Inc., New York, 1969), 2nd ed., p. 233.
- 6) See Ref. 5, p. 235.
- 7) R. T. Weidner and R. L. Sells, Elementary Modern Physics (Allyn and Bacon, Inc., Massachusetts, 1960), p. 213.
- 8) M. J. Martin and P. H. Blichert-Toft, Nucl. Data A. 8, 5 (1970).
- 9) C. M. Lederer, J. M. Hollander, and I. Perlman, Table of Isotopes (John Wiley and Sons, Inc., New York, 1968), 6th ed., p. 570.
- 10) J. A. Bearden, Handbook of Chemistry and Physics (The Chemical Rubber Co., Ohio, 1969), 50th ed., p. E-156.
- 11) See Ref. 10, p. E-157.
- 12) E. Merzbacher and H. W. Lewis, Handbuch der Physik (Springer-Verlag, Berlin, 1958), Vol. 34, Chap. A, p. 166.
- 13) See Ref. 5, p. 244.
- 14) P. Richard, I. L. Morgan, T. Furuta, and D. Burch, Phys. Rev. Lett. 23, 1009 (1969).
- 15) T. B. Johansson, R. Akselsson, and S. A. E. Johansson, Nucl. Instr. Meth. 84, 141 (1970).
- 16) R. J. Fortner, B. P. Curry, R. C. Der, T. M. Kavanagh, and J. M. Khan, Phys. Rev. 185, 164 (1969).
- 17) See Ref. 15, p. 141.
- 18) See Ref. 15, p. 143.

ACKNOWLEDGMENTS

The author wishes to express his appreciation to Dr. G. G. Seaman who suggested the project and has been more than patient with the giving of his time and assistance.

The author is also grateful for the help of Dr. C. E. Rosenkilde in the writing of this thesis.

ANALYSIS OF SURFACE CONTAMINANTS IN BIOLOGICAL
SAMPLES BY CHARACTERISTIC X-RAY ANALYSIS

by

MONTY O. VOLCKMANN

B. S., Southwest Missouri State College, 1970

AN ABSTRACT OF A MASTER'S THESIS

submitted in partial fulfillment of the

requirements for the degree

MASTER OF SCIENCE

Department of Physics

KANSAS STATE UNIVERSITY
Manhattan, Kansas

1972

ABSTRACT

Lead and Mercury contaminants in flour samples were detected by observing K-series characteristic X-rays following bombardment by protons. A sensitivity of 100 parts per million was obtained for lead from a thick target of flour. Thick targets were used since many substances are more conveniently prepared for analysis in this form. A sensitivity of one part per ten million should be obtainable by observing L-series X-rays. This technique should be useful in determining the amount of heavy element contaminants in food and food substances.